Research Article

BIOMEDICAL Journal of Scientific & Technical Research

ISSN: 2574 -1241

DOI: 10.26717/BJSTR.2024.56.008895

Acidic and Basic Proteins from Spider Latrodectus Pallidus Venom that Induce Formation of Non-Bilayer Phase and Increase Proton Capacity in Model Myelin Membranes Feature High Sequence Homology to Isoforms of Myelin Basic Protein: Pharmacological Relevance

Anwaar S Chaudary[1], Chenchang Jiang[1], Yanglin Guo[1] and Edward S Gasanoff[1,2]*

[1]*STEM Research Center, Chaoyang Kaiwen Academy, China*

[2]*Belozersky Institute of Physico-Chemical Biology, M.V. Lomonosov Moscow State University, Russia*

***Corresponding author:** Edward S Gasanoff, STEM Research Center, Chaoyang Kaiwen Academy, 100018 Beijing, China and Belozersky Institute of Physico-Chemical Biology, M.V. Lomonosov Moscow State University, 119991 Moscow, Russia

ARTICLE INFO

Received: May 15, 2024

Published: May 23, 2024

Citation: Anwaar S Chaudary, Chenchang Jiang, Yanglin Guo and Edward S Gasanoff. Acidic and Basic Proteins from Spider Latrodectus Pallidus Venom that Induce Formation of Non-Bilayer Phase and Increase Proton Capacity in Model Myelin Membranes Feature High Sequence Homology to Isoforms of Myelin Basic Protein: Pharmacological Relevance . Biomed J Sci & Tech Res 56(4)-2024. BJSTR. MS.ID.008895.

ABSTRACT

This study describes the isolation of novel acidic and basic proteins from the venom of the Latrodectus pallidus (white widow spider), which exhibit high amino acid sequence homology to the 18.5 kDa isoforms of myelin basic proteins. This study explores the ability of model myelin membranes, composed of phospholipids and the acidic and basic proteins from spider venom, to absorb protons and form a non-bilayer lipid phase. The results of this study support a previously suggested concept by A.M. Morelli, which proposes that the myelin membrane may accumulate protons on its surface to store energy. The energy stored on membrane surface could then be used to drive proton circuits, potentially coupling hypothetical redox processes and ATP synthesis within the myelin membrane.

Introduction

Spiders evolved over 300 million years ago, and through their long evolutionary history, spiders developed into animals with well-equipped venoms comprising a great variety of biochemical compounds designed to paralyze and/or kill their prey, rendering spiders the most successful venomous creatures in evolution [1]. Proteins constitute a major portion of spider venoms that display diverse pharmacological activities, representing vast evolutionary-edited natural pharmacopoeias that attract research efforts leading to the potential development of novel pharmaceuticals [2,3]. A few spider venom protein toxins have been used as invaluable ligands targeting

various pharmacological targets. Some of these venom protein toxins are now undergoing preclinical and clinical studies for the treatment of multiple sclerosis, diabetes, and cardiovascular pathologies [4]. Spider venom proteins are also used in fundamental studies as crucial tools for probing electrophysiological processes in biological membranes [2]. For example, hanatoxins from Grammostola rosea and agatoxins from Agelenopsis aperta have been used as specific ligands of voltage-gated potassium and calcium channels [5,6]. In addition, spider venoms comprise a variety of stable small proteins with strong insecticidal activity that cause paralysis and/or lethality of insects by affecting ion channels, receptors, and enzymes [7]. This kind of research on the insecticidal activity of spider venom proteins holds high potential for the development of novel bioinsecticides, which are finding applications in green agricultural biotechnology [8,9].

The venoms of Latrodectus widow spiders, a genus of spiders in the family Theridiidae erected by Charles Athanase Walckenaer in 1805 [10], are probably the most studied spider venoms due to their extraordinary potent neurotoxins [11,12], which draw not only medical interest but also the general interest of scholars who use Latrodectus neurotoxins in studies of molecular mechanisms in neurobiology and pharmaceutical research [13]. The spiders of the Latrodectus genus comprise 32 species spread around the globe [14-16], with most of the species found in South and North Americas [10,17]. The most potent Latrodectus neurotoxin is α-latrotoxin, which targets the vertebrate central nervous system by attacking the presynaptic membrane of neurons, leading to increased intracellular Ca^{2+} concentration that triggers elevated exocytosis of neurotransmitters in the intermembrane synaptic cleft [13,18]. The less potent Latrodectus neurotoxins are α, β, γ, δ, ε-latroinsectotoxins, which bind to specific receptors on the presynaptic membrane of neuronal cells of insects, and α-latrocrustatoxin, which attacks the presynaptic membrane of crustaceans [18].

Overall, the neurotoxic activity of 'latro-insecto-crusta-toxins' is based on the binding of toxins to neuronal cells, which promotes the release of neurotransmitters either via stimulating exocytosis or through the formation of transmembrane tetrameric pores promoting specific Ca^{2+} permeability [18]. Noteworthy, it has been reported earlier that α-latroinsectotoxin from Latrodectus mactans venom promotes the conductivity of bilayer lipid membranes in the ion channel manner for divalent cations in the following order of decreasing permeability $Ba^{2+} > Ca^{2+} > Mg^{2+} > Cd^{2+} > Zn^{2+}$ [19]. Besides the neurotoxins, Latrodectus venoms have been reported to contain metalloproteases, serine proteases, chitinases, hyaluronidases, venom allergen antigen 5-like proteins, etc. [13]. In addition, cationic proteins with antibacterial activity have been detected in Latrodectus geometricus venom [20]. In a recent study, the chromosome-level genome assembly of Latrodectus elegans spider venom with 55 identified toxin genes has been reported [21], which is more than the number of different types of venom proteins identified in all studied species of the Latrodectus genus. This finding suggests that there are still more unknown proteins to be identified in the venom of spiders of the Latrodectus genus.

The venom of Latrodectus pallidus, the white widow spider, which inhabits the deserts of Central Asia, is the least studied venom among species of the Latrodectus genus [22]. In 2014, the venom from Latrodectus pallidus was fractionated to reveal that, in addition to the types of proteins commonly found in venoms of the Latrodectus genus, such as α-latrotoxin, latrodectin, latroinsectotoxin, phospholipase D, hyaluronidase, and serine protease, there are two proteins, one acidic and another basic, both of 18.5 kDa, in the Latrodectus pallidus venom. These proteins have amino acid sequences which are not homologous to the amino acid sequences of proteins previously identified in venoms of the Latrodectus genus [22]. Interestingly, the amino acid sequences of the two proteins of 18.5 kDa from the Latrodectus pallidus venom are highly homologous to the sequences of myelin basic protein isoforms. In the present study, we used the Latrodectus pallidus venom acidic and basic proteins of 18.5 kDa as the protein component of the model myelin membrane, which included, as the lipid component, the major phospholipids of the myelin membrane, such as sphingomyelin, phosphatidylethanolamine, phosphatidylserine, phosphatidylinositol, and phosphatidylcholine, to examine the proton absorbing capacity and the polymorphic phospholipid transitions in the model myelin membrane. The results obtained in the present study support the innovative proposal that outlines the novel biological function of the myelin membrane related to the accumulation of protons on the myelin membrane surface to serve a function of proton capacitor, a novel concept suggested by Professor Alessandro M. Morelli [23]. The results of the present study also propose new tentative physiological roles for phospholipids and acidic and basic proteins of the myelin membrane.

Materials and Methods

Chromatography

The lyophilized venom from the Central Asian white widow spider Latrodectus pallidus was a gift from Prof. L. Ya. Yukelson (Institute of Biochemistry, Uzbekistan Academy of Sciences). The venom (200 mg) was dissolved in 1.5 ml of 5.0 mM Tris-HCl, pH 8.0 buffer and applied onto the cation-exchange CM Sephadex C-50 (Nanjing Duly Biotech Co. Ltd, Nanjing, China) borosilicate column (1.5 × 35 cm) equilibrated overnight in 5.0 mM Tris-HCl, pH 8.0 buffer at 25°C. The KCl gradient in the same buffer was administered as shown in Figure 1. Acidic protein was collected from the shaded area of F1 peak (Figure 1), then dialyzed against water in 1.0 kDa cutoff dialysis tube (Sigma Aldrich, Saint Louis, USA) and lyophilized on the vacuum freeze-drying lyophilizing machine YTLG-10 (Shanghai Yetuo Co., Ltd., China) at 2 Pa and −60°C for 12 hours. A sample from shaded area in F7 peak (Figure 1) was dialyzed and lyophilized as described above and then sub-fractionated by cation-exchange HPLC in a SynChropak S300 column. A 20 mg/ml sample was dissolved in 0.02 M Bis-Tris, pH 7.3 and injected into a SynChropak S300 column and a

linear gradient was established with 0.5 M HCl buffer 5 min after the sample was injected. Basic protein was collected after 17 min elution time as shown by shaded area in Figure 2. The basic protein was dialyzed and lyophilized as described above.

Electrophoresis

SDS-polyacrylamide gel electrophoresis was carried out on the Mini-PROTEAN Tetra Vertical Electrophoresis Cell using Mini-PROTEAN TGX precast 12% density gels (Bio-Rad Laboratories Co., Ltd., Shanghai, China). Protein samples were dissolved in 20mM Tris-HCl pH 7.0 buffer with 2 mM EDTA, 5% SDS, 10% DDT, 0.01% Bromophenol Blue, 2% glycerol at a final protein concentration 2 mg/ml and boiled for 10 min. A 15 µl portion of each protein sample and low molecular weight markers for SDS-PAGE (Thermo Fisher Scientific Inc., Shanghai, China) were applied into wells of the precast 12% density gel. The running buffer was 500 ml 1×TAE (Tris-acetate-EDTA) pH 7.0 including 7.2 g glycine and 0.2 g SDS. Electrophoresis proceeded for 50 minutes at 100 V. Isoelectric focusing (IEF) was carried out on the horizontal plate Isoelectric Focusing apparatus DYCP-37B (Beijing Liuyi Biotechnology Co., Ltd., China) using the Ready Gel Precast Gel with ampholyte of pH range 3–10.5 and the protein markers for IEF with pI range of 4.65–10.6 (Shanghai Yeyuan Biotechnology Co., Ltd., China). The pH gradient in the precast IEF gel was adjected by running electric power at 75 V for 30 minutes after which 5 µl of each protein sample (1mg/1ml H_2O) and IEF protein markers were applied onto the precast IEF gel and the power of 90 V was run for 120 minutes.

Amino acid residues sequencing: The detailed protocol for resolving the sequences of amino acid residues of acidic and basic proteins purified from the Central Asian white widow spider Latrodectus pallidus was described previously [22]. Briefly, the amino acid composition of proteins was determined with the High-Speed Amino Acid Analyzer LA8080 AminoSAAYA (Hitachi High-Tech, Shanghai Co., Ltd., China). Reduction and carboxymethylation of proteins were conducted as previously described [24]. Proteins were hydrolyzed for 5 hours at 37°C with trypsin at 1:50 w/w protein to trypsin ratio. The carboxymethylated protein hydrolysate was chromatographed on Chromo-Beads resin (Koram Biotech Corp., Seul, Korea) and then further purified by paper electrophoresis and chromatography. The amino acid sequence of the protein fragments was determined as described previously [25]. The carboxymethylated proteins were incubated for 20 hours at 25°C in 70% formic acid. The cyanogen bromide cleavage was done using a 100-fold excess of reagent. The products of the carboxymethylation and cyanogen bromide cleavage were purified on Sephadex G-25 in 0.1 M NH_4–HCO_3 buffer. Paper chromatography was used to isolate the chymotryptic peptides of the cyanogen bromide fragment of proteins.

The N-terminal sequences of carboxymethylated proteins and the cyanogen bromide fragment forming the C-terminus of the original proteins were resolved on a Beckman model 890C sequencer (Beckman Instruments Inc., Fullerton, CA, USA) and the C-terminus sequence was resolved by means of carboxypeptidase A. Total lipid extract isolation and purification: Wistar rat liver was homogenized in a Warning Blender 700G for 3 minutes in 300 ml chloroform and 200 ml methanol, then100 ml of methanol and 200 ml dd-H_2O was added and the mixture was blended for another 5 minutes. Homogenate was centrifuged at 200 g for 20 minutes and aqueous layer of methanol and dd-H_2O was discarded. The chloroform phase with lipids was washed with 300 ml saline and centrifuged at 200 g for 15 minutes after which saline layer was discarded, and the chloroform phase was washed two more times. The lipids in chloroform were filtrated through the Whatman No.1 filter paper and the lipids were washed from the filter paper with 30 ml methanol.

Preparation of phospholipid specific polyvalent antibodies: Polyvalent antibodies specific for the selected phospholipids were developed using adult male Wistar rats. The adjuvant-primed animals received injections of the synthetic polar heads of phospholipids: one animal was injected with one type of phospholipid polar head. The synthetic polar heads of phosphatidylethanolamine, phosphatidylcholine, phosphatidylinositol, phosphatidylserine and sphingomyelin were from NOF America Co., White Plains, USA. Ascites fluids were collected from the peritoneal cavity of animals two weeks after injection. The polyvalent antibodies from ascites fluids were purified on a Protein-A-Sepharose column (Pharmacia, Uppsala, Sweden). Purification of individual phospholipids by immunoaffinity chromatography: The borosilicate columns for immunoaffinity chromatography were loaded with the Sephadex G-25 resin containing covalently linked antibodies specific to the polar heads of either phosphatidylserine, sphingomyelin, phosphatidylinositol, phosphatidylcholine or phosphatidylethanolamine with each column containing only one type of antibodies, so overall five different immunoaffinity columns were prepared.

The antibodies were covalently linked to the Sephadex G-25 resin using Pierce™ Traut's Reagent 2-iminothiolane Kit and N-succinimidyl 3-(2-pyridyldithio)propionate Kit (Thermo Fisher Scientific Inc., Shanghai, China) according to the manufacture's protocol. The Sephadex G-25 resin with linked antibodies was equilibrated in 1.0 mM Tris-HCl, pH 7.0 buffer at 25°C for three hours. A 5 ml portion of the concentrated total lipid extract in methanol was applied into each of five immunoaffinity columns and the individual phospholipid fractions eluted from the columns were pulled into tubes with 15 ml chloroform and centrifuged at 200 g for 15 minutes to discard aqueous layer. Chloroform from the tubes was removed by drying with vacuum pump for one hour. The mass of phospholipid obtained was determined as the different in mass between the tube with dry phospholipid and the same empty tube. The concentration of stock solutions of phospholipids in chloroform of 0.1 M was prepared assuming molecular masses of phospholipids: 716 g/mol for phosphatidylethanolamine, 887 g/mol for phosphatidylinositol, 768 g/mol for phosphatidylcholine, 792 g/mol for phosphatidylserine and 734 g/mol for sphingomyelin.

Preparation of unilamellar liposomes: The unilamellar phospholipid liposomes for the studies of ability of liposomal membrane to absorb protons, that is to serve as protons capacitor, were prepared by the treatment of aqueous lipid dispersions with ultrasonic wavelength frequency. Aliquots of phospholipids in chloroform containing molar ratio 4 to1 of phosphatidylcholine and either phosphatidylethanolamine, phosphatidylserine, sphingomyelin or phosphatidylinositol were dried with vacuum pump for 5 hours at 25°C for complete removal of chloroform, that is until the chloroform free phospholipid films were formed. Phospholipid films were then hydrated with dd-H_2O pH 7.0 at phospholipid concentration 10^{-5} M and the resulted phospholipid dispersion was sonicated with the Ultrasonic Dispenser Yt-JY96-IIN (Shanghai Yetuo Technology Co., Ltd., China) at 22 kHz in helium atmosphere for 15 minutes at 4°C. Liposomes were then incubated for 15 hours at 15°C. The unilamellar phospholipid liposomes modified by acidic and basic proteins were prepared by adding equal molar amounts of acidic and basic proteins into the liposome sample at a total protein concentration 2×10^{-7} M.

To prevent electrostatic interaction of acidic and basic proteins in solution, the acidic protein was added first to liposome samples and incubated for 15 minutes with the continuous stirring of liposome solution with the magnetic stirrer JB-3 (Shanghai INESA Scientific Instruments Co. Ltd., China). Then the basic protein was added to the liposomes which were already modified by acidic protein and liposomes were incubated for another 15 minutes. The pH readings were taken in pure dd-H_2O, in liposome samples and in liposome samples modified by the acidic and basic proteins. For the sake of uniform pH readings, all liposome samples treated or untreated with the proteins were continuously stirred with the magnetic stirrer. The proton concentration in pure dd-H_2O and liposome samples treated or untreated with the proteins were determined from the measured pH values by using the following conversion: [H+] = 10–pH. 1H-NMR studies of unilamellar liposomes: For the ^{1}H-NMR studies $2H_2O$ was used instead of dd-H_2O to prepare sonicated unilamellar liposomes according to protocol described above. Phospholipid concentration in liposomes for the 1H-NMR studies was 1.4×10^{-2} M and protein concentration was 1.75×10^{-4} M. Liposomes were treated with 10 µl of saturated K3Fe(CN)6 solution per 1 ml of liposomes. 1H-NMR spectra from $N+(CH_3)_3$ groups of unilamellar liposomes were recorded using a Varian XL-200 spectrometer (USA) at an operating frequency of 200 MHz at 25°C. The width of the 90° pulse was 8.7 µs, the relaxation delay was 50 µs and the acquisition time for free induction signal was 1 s. The integral intensity of ^{1}H-NMR signals from choline groups was measured in triplicate and variation among triplicate readings was never higher than 6%.

Statistics: For each data point coming from the pH readings of dd-H_2O and the liposome samples, they were prepared in triplicate, and the standard deviation between the readings was within 0.09% of the means. The pH readings coming from the four types of liposome samples and from the dd-H2O sample were statistically compared by using an ANOVA test. For statistical comparison of pH readings between liposome samples and liposome samples treated with proteins, the T-test was used. The p-values less than 0.05 were considered as statistically significant differences.

Results

We fractionated the Central Asian spider Latrodectus pallidus venom by the cation-exchange column chromatography to purify acidic and basic proteins. We used one column to purify acidic protein and two columns to purify basic protein. The chromatograms derived from the two column fractionations are shown in Figure 1. Acidic protein was collected from the shaded area of the F1 peak in the chromatogram obtained by fractionation on the CM Sephadex C-50 column (Figure 1A). To isolate the basic protein, a fraction of proteins was collected from the shaded area of the F7 peak (Figure 1A), and this fraction of proteins was then sub-fractionated by cation-exchange HPLC in a SynChropak S300 column. The basic protein was isolated from the shaded area of the fraction shown in Figure 1B. Both the acidic and basic proteins were homogeneous by SDS-PAGE and isoelectric focusing electrophoresis (Figure 2). The molecular mass of both proteins was somewhat below 21.1 kDa, and the pI values were around 4.65 and slightly above 10.6 for the acidic and basic proteins, respectively. The amino acid sequences of the acidic and basic proteins, which were resolved according to the protocol described in the Materials and Methods, are aligned in Figure 3.

DOI: 10.26717/BJSTR.2024.56.008895

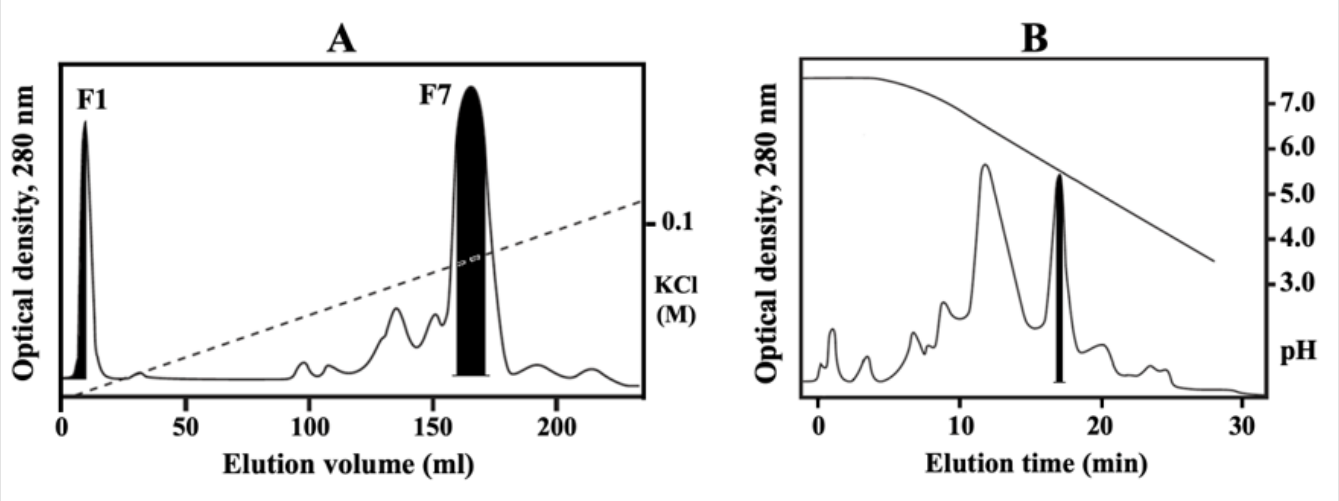

Figure 1: A – Cation-exchange column (1.5 × 35 cm) chromatography of Central Asian spider Latrodectus pallidus venom. A sample (200 mg) was applied onto CM Sephadex C-50 in 5.0 mM Tris-HCl, pH 8.0 buffer with KCl gradient as shown by broken line. Acidic protein was collected from area of F1 shaded black. A mixture of proteins was collected from area of F7 shaded black. B – Subfractionation of a mixture of proteins from F7 by cation-exchange HPLC. A sample (20 mg/ml) dissolved in 0.02 M Bis-Tris, pH 7.3 was injected into a SynChropak S300 column and a linear gradient was established with buffer containing 0.5 M HCl 5 min after the sample was injected. Basic protein was collected after about 17 min elution time as shown by area shaded black.

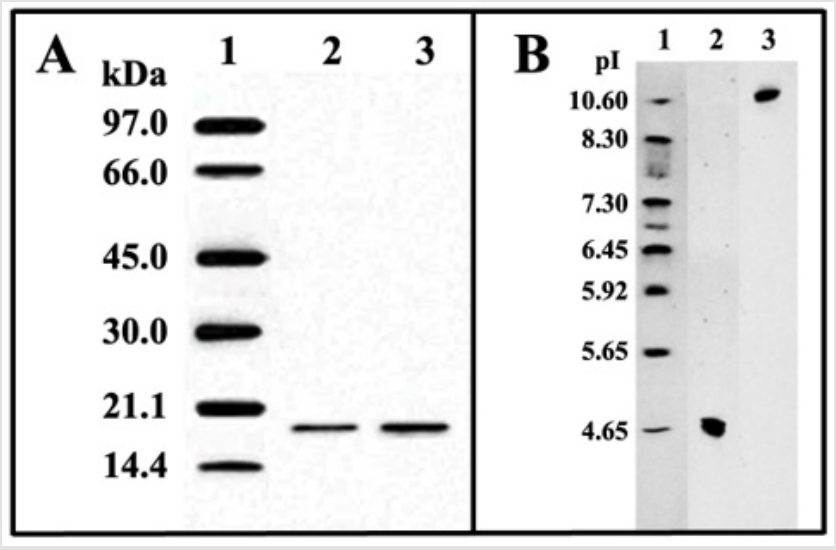

Figure 2:

A. SDS-polyacrylamide 12% gel electrophoresis of acidic protein (lane 2) and basic protein (lane 3) isolated from the Central Asian spider Latrodectus pallidus venom. Lane 1 carries the standard low molecular weight markers.

B. Isoelectic focusing (IEF) of the of acidic protein (lane 2) and basic protein (lane 3) isolated from the Central.

Asian spider Latrodectus pallidus venom in the Ready Gel Precast Gels with ampholytes of pH gradient from 3.0 to 10.5. The standard markes from the FMC Corporation (Rockland, ME, USA) with pI range from 4.65 to 10.6 are on the lane 1.

DOI: 10.26717/BJSTR.2024.56.008895

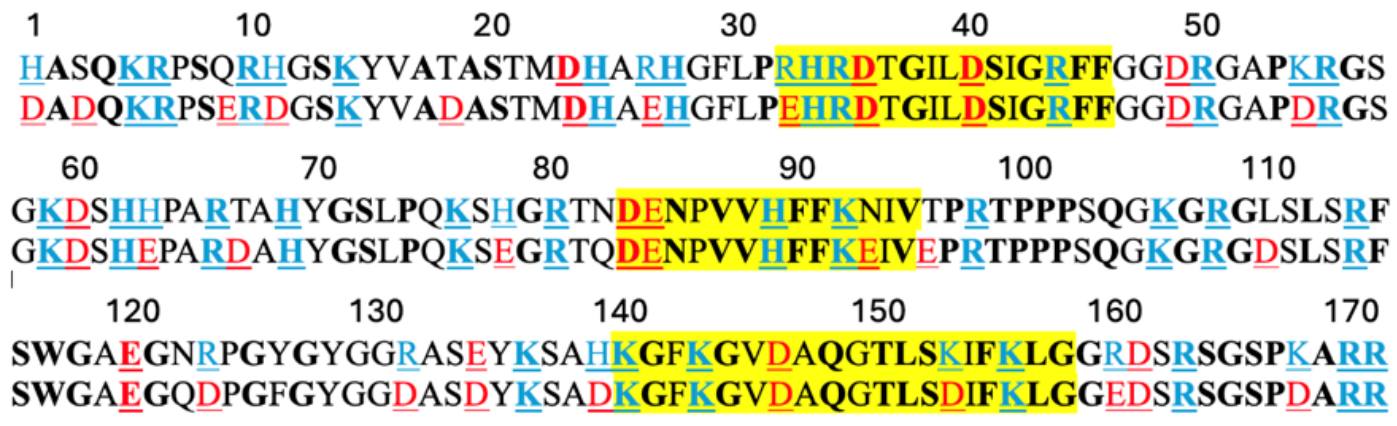

Figure 3: Alignment of amino acid sequences of basic (top sequence) and acidic (bottom sequence) proteins isolated from venom of Central Asian spider Latrodectus pallidus. Amino acid sequences of both proteins are homologues to the human myelin basic protein isoforms with the 100% sequence homology in the highly conserved regions shown in bold letters [25]. The regions highlighted in yellow fold into α-helical structures when proteins tightly attach to the membrane [26]. Charged residues are underlined and blue letters indicate positively charged residues and red letters negatively charged residues.

Amino acid sequences of both proteins are highly homologous to the human myelin basic protein isoforms [26]. In addition, both acidic and basic proteins show 100% sequence homology to the myelin basic protein isoforms from various species in the highly conserved amino acid sequence regions [27] (Figure 3). The calculated molecular mass and the isoelectric points of the Latrodectus pallidus venom acidic and basic proteins match exactly the most abundant isoforms in the adult human myelin with molecular mass 18.5 kDa [26]. These findings prompted us to use acidic and basic proteins in the studies of electrophysiological and structural properties of model myelin membrane. We have incorporated acidic and basic proteins from the Latrodectus pallidus venom into the model myelin membrane to investigate whether the model myelin membrane can absorb protons on its surface from the bulk water and undergo polymorphic phospholipid transitions.

The myelin membrane in the vertebrate central nervous system is mostly made of five phospholipids: phosphatidylcholine (PC), phosphatidylethanolamine (PE), phosphatidylserine (PS), phosphatidylinositol (PI), and sphingomyelin (SM) [28-31]. In terms of the protein component of the membrane, the isoforms of myelin basic protein are one of the most abundant components of the myelin membrane, the primary role of which is to maintain a compact myelin sheath [32]. PC is the dominant phospholipid that stabilizes the bilayer structure in most, if not all, biological membranes, including the myelin membrane [32-34]. The role of the other four phospholipids is not clear, but it has been suggested that each of those phospholipids plays a particular purpose in the functional activities of the myelin membrane [32]. In the present work, for the studies of proton absorption by the membrane surface, we have prepared four types of model myelin membranes, each of which includes PC and one of the four phospholipids of a particular function with the molar percentage ratio of 80% for PC and 20% for either PE, PS, PI, or SM, with a total phospholipid concentration of 10^{-5} M.

For the protein component of the four types of model myelin membrane, the total protein concentration of acidic and basic proteins of an equal molar ratio was 2×10^{-7} M. For the studies of polymorphic transitions of phospholipids in the model myelin membranes, we prepared the same four types of myelin membranes with the molar percentage ratio of 80% for PC and 20% for one of the phospholipids of a functional group, but we used different total phospholipid and protein concentrations, which were 1.4×10^{-2} M for phospholipids and 1.75×10^{-4} M for proteins. The model membrane system for myelin membranes was unilamellar liposomes, both for the studies of proton absorption by the membrane surface and for the studies of polymorphic phospholipid transitions. To assess the absorbance of protons by the myelin membrane liposomes, we measured the difference between pH values in pure dd-H_2O and in dd-H_2O solutions of liposomes from four models of myelin membranes, which did not include acidic and basic proteins (Table 1).

Table 1: The pH readings taken in triplicate at 25°C in dd-H_2O and in dd-H_2O solutions of liposomes made of either phosphatidylcholine (PC) + phosphatidylserine (PS), phosphatidylcholine + phosphatidylinositol (PI), phosphatidylcholine + phosphatidylethanolamine (PE) or phosphatidylcholine + sphingomyelin (SM). The mean values of pH readings, standard deviations (SD) and the ANOVA p-value are also given in the Table 1. The concentration of phospholipids in all samples is 10^{-5} M.

	The pH values	Means	SD	ANOVA *p*-value
dd-H_2O	7.01 6.99 7.00	7.00	0.0082	4.0389×10^{-7}
PC+PS	7.16 7.19 7.19	7.18	0.0141	
PC+PI	7.17 7.14 7.14	7.15	0.0141	
PC+PE	7.11 7.11 7.14	7.12	0.0141	
PC+SM	7.09 7.08 7.10	7.09	0.0082	

Preparations of liposomes in dd-H_2O produced basic pH values (pH above 7.0), which is a result of protein absorption by the surface of the liposomal membrane. As shown in Table 1, the PS-containing membrane (PC+PS) demonstrates the highest change in pH towards basic values (7.18), indicating that the PC+PS membrane is the strongest proton capacitor among the four models of myelin membranes. This is due to the two acidic moieties, carboxyl and phosphate groups, in the PS polar head (Figure 4). Although the other three model myelin membranes each contain one of the 'functionally-driven' phospholipids (PI, PE, or SM), all of which have only one acidic moiety (phosphate group) in their polar heads, their proton absorption abilities differ and decrease in the following order: PI – pH 7.15, PE – pH 7.12, and SM – pH 7.09. The highest ability of PI to absorb protons among the three 'functional' phospholipids can be explained by the polar hydroxyl groups of the inositol moiety in the polar head of PI (Figure 4), which have the potential to absorb protons via the formation of coordinate bonds with the lone pair of electrons on the oxygen atoms of the hydroxyl groups.

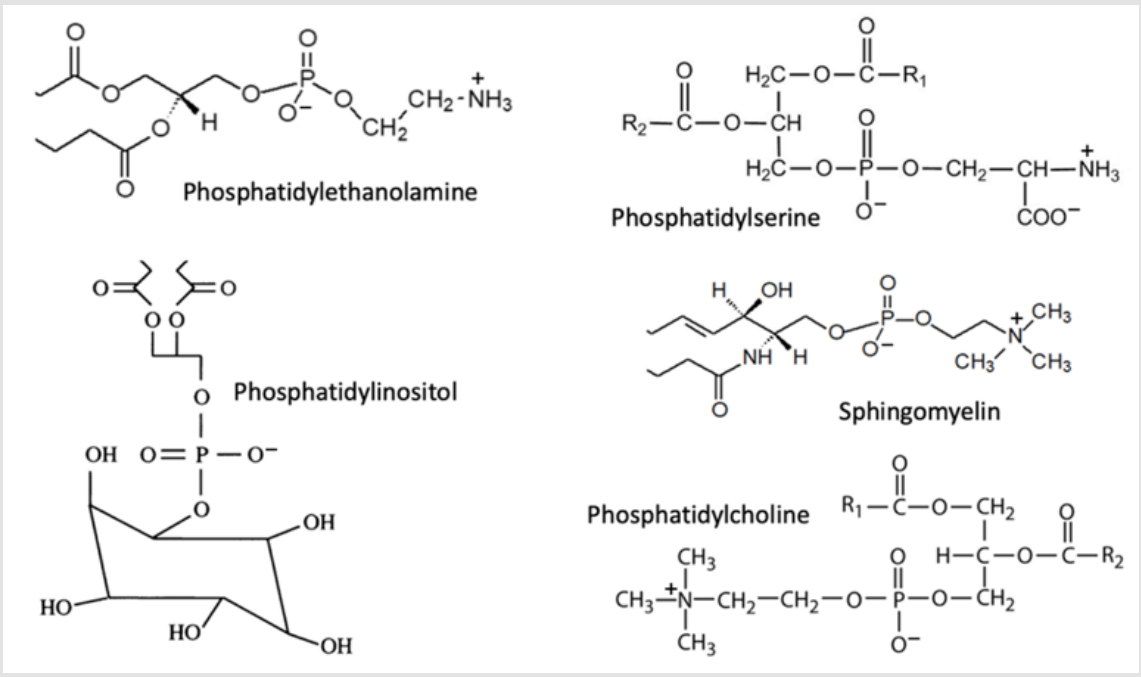

Figure 4: The structural formulars of polar head groups of phosphatidylethanolamine, phosphatidylserine, phosphatidylinositol, sphingomyelin and phosphatidylcholine.

The higher ability of PE to absorb protons compared to SM can be attributed to the larger size of the choline group ($-N^+(CH_3)_3$) in SM versus the amino group ($-N^+H_3$) in PE (Figure 4). The smaller size of the amino group allows better access for protons to the phosphate group of PE than the choline group of SM. It should be noted that the ANOVA p-value for the statistical differences in pH values is very small within the group including pure dd-H_2O and dd-H_2O solutions of the four models of myelin liposomal membranes, indicating that the differences are statistically significant. The effect of the equimolar mixture of acidic and basic proteins (Pr) incorporated into the four models of myelin liposomal membranes is shown in Table 2. In all four membrane models, the incorporation of Pr resulted in a further increase in pH values, demonstrating that Pr contributes to the proton absorption of the myelin membrane. Thus, Pr enhances the myelin membrane's ability to act as a proton capacitor. The largest increase in pH value (1.05) triggered by Pr was observed in the PS-containing membrane. The second largest increase in pH value (1.03) was observed in PE-containing membranes.

Table 2: Comparison of pH values in samples of liposomes made of either phosphatidylcholine (PC) + phosphatidylserine (PS), phosphatidylcholine + phosphatidylinositol (PI), phosphatidylcholine + phosphatidylethanolamine (PE) or phosphatidylcholine + sphingomyelin (SM) and the same liposomes treated with a mixture of acidic and basic proteins (Pr). The pH readings mean values, standard deviations (SD) and the T test p-values are also given in the Table 2. The concentrations of phospholipids and Pr are 10^{-5} M and 2×10^{-7} M respectively.

PC+PS liposomes Against PC+PS+Pr liposomes				
	The pH values	**Means**	**SD**	**T test p-value**
PC+PS	7.16 7.19 7.19	7.18	0.0141	8.7684×10^{-8}
PC+PS+Pr	8.23 8.22 8.24	8.23	0.0082	
PC+PE liposomes against PC+PE+Pr liposomes				
	The pH values	Means	SD	T test p-value
PC+PE	7.11 7.11 7.14	7.12	0.0141	2.1296×10^{-7}
PC+PE+Pr	8.17 8.14 8.14	8.15	0.0141	
PC+PI liposomes against PC+PI+Pr liposomes				
	The pH values	Means	SD	T test p-value
PC+PI	7.17 7.14 7.14	7.15	0.0141	7.9841×10^{-7}
PC+PI+Pr	7.87 7.90 7.90	7.89	0.0141	
PC+SM liposomes against PC+SM+Pr liposomes				
	The pH values	Means	SD	T test p-value
PC+SM	7.09 7.08 7.10	7.09	0.0082	8.2504×10^{-7}
PC+SM+Pr	7.76 7.78 7.74	7.76	0.0163	

The increase in pH value triggered by Pr in PC+PI and PC+SM was significantly lower, at 0.74 and 0.67, respectively. The very low T-test p-values comparing the statistical differences between pH values in model myelin membranes not containing Pr and those containing Pr confirm that the increases in pH values triggered by Pr are statistically significant. To better present the differences in proton capacitor power between the four models of myelin membranes in the absence and presence of Pr, the concentrations of absorbed protons are shown in Figure 4 as the negative logarithm of [H+] absorbed by the model myelin membranes. It should be noted that the lower the negative logarithm of [H+] value, the higher the concentration of H+ ions absorbed. Thus, by comparing the heights of the bars in Figure 4, one can conclude that the myelin membranes containing Pr exhibit higher proton capacitor power than myelin membranes without Pr. Additionally, one can conclude that among the myelin membranes containing Pr, the PC+PS and PC+PE membranes have a higher proton absorbing capacity than the PC+PI and PC+SM membranes (Table 3).

Table 3: The concentration of H^+ ions in dd-H_2O (initial H^+ concentration), concentration of H+ ions after adition of proteins, liposomes or liposomes modified with proteins to dd-H_2O (final H+ concetration) and concentration of H^+ ions absorbed by proteins, liposomes or liposomes modified with proteins (absorbed H^+ concentration). Concentrations of phospholipids and proteins in liposome samples are 10^{-5} M and 2×10^{-7} M respectively. Pr – mixture of acidic and basic proteins, PC – phosphatidylcholine, PS – phosphatidylserine, PE – phosphatidylethanolamine, PI – phosphatidylinositol, SM – sphingomyelin. Column –log [H^+] shows negative logarithm values of absorbed [H^+].

Samples added to dd-H_2O	**Initial [H^+] (M)**	**Final [H^+] (M)**	**Absorbed [H^+] (M)**	**–log [H^+]**
Pr	1×10^{-7}	3.55×10^{-8}	6.45×10^{-8}	7.19
PC+PS	1×10^{-7}	6.61×10^{-8}	3.39×10^{-8}	7.47
PC+PS+Pr	1×10^{-7}	5.89×10^{-9}	9.41×10^{-8}	7.03
PC+PE	1×10^{-7}	7.59×10^{-8}	2.41×10^{-8}	7.62
PC+PE+Pr	1×10^{-7}	7.08×10^{-9}	9.29×10^{-8}	7.03
PC+PI	1×10^{-7}	7.08×10^{-8}	2.92×10^{-8}	7.54
PC+PI+Pr	1×10^{-7}	1.28×10^{-8}	8.72×10^{-8}	7.06
PC+SM	1×10^{-7}	8.13×10^{-8}	1.87×10^{-8}	7.73
PC+SM+Pr	1×10^{-7}	1.74×10^{-8}	8.26×10^{-8}	7.08

To study the permeability and polymorphic transitions of phospholipids in the four models of myelin membranes in the absence and presence of Pr, we used 1H-NMR spectroscopy of unilamellar liposomes in the presence of $K_3[Fe(CN)_6]$. The methodology and advantages of unilamellar liposome 1H-NMR spectroscopy with paramagnetic $Fe(CN)_6^{3-}$ ions are described in detail in our previous publications [35-38]. Briefly, $Fe(CN)_6^{3-}$ ions interact with the choline ($N+(CH_3)_3$) groups of the outer monolayer of the liposomal membrane, shifting the choline signal of the outer monolayer to higher values of the applied magnetic field, while the signal of the choline groups from the inner monolayer remains unchanged. This results in the splitting of 1H-NMR signals from the outer and inner monolayers of the liposomal membrane. Should the liposomal membrane become permeable to $Fe(CN)_6^{3-}$ ions, which would allow interaction with the choline groups of the inner membrane, the signal of the choline groups from the inner monolayer would shift to the field of the outer monolayers, causing the inner monolayer signal to visually disappear.

As shown in Figure 5, all four model myelin liposomal membranes in the absence of Pr were not permeable to $Fe(CN)_6^{3-}$ ions. The higher intensity of the 1H-NMR signals in the PC+SM liposomes compared to the other three types of liposomes is due to both PC and SM having a choline group in their polar heads, while in the other three types of liposomes, only PC has a choline group. The addition of Pr to the liposome samples resulted in the broadening of 1H-NMR signals due to the restriction of molecular mobility of lipids by Pr. However, the addition of Pr did not make the membrane in any of the four liposome samples permeable to $Fe(CN)_6^{3-}$ ions, as the signals from the inner monolayers remained intact. Notably, in the PC+PS+Pr and PC+PE+Pr liposomes, a small signal appeared in the higher field from the signal of the outer monolayer (Figure 5). This signal originated from the formation of a non-bilayer lipid phase [35-38] and was more pronounced in the PC+PE+Pr membrane. The formation of the non-bilayer lipid phase in model membranes containing PS and PE, triggered by interaction with basic proteins, was observed previously [35,38-41]. It is evident that the non-bilayer lipid phase in model myelin membranes containing PS or PE was induced by the basic protein from the white widow spider venom (Figures 5 & 6).

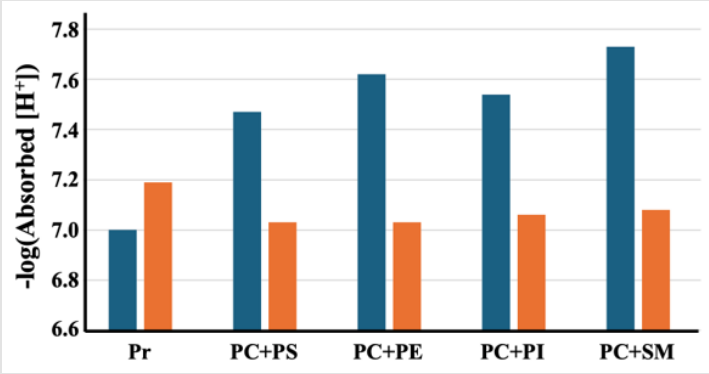

Figure 5: Negative logarithm of absorbed [H^+] by acidic and basic proteins (Pr) in dd-H2O, by liposomes only and by liposomes treated with Pr. Emerald bars: -log[H^+] in dd-H_2O, -log[H^+] absorbed by liposomes made of PC+PS, PC+PE, PC+PI and PC+SM. Orange bars: -log[H^+] absorbed by Pr in dd-H_2O and by liposomes treated with Pr. PC – phosphatidylcholine, PS – phosphatidylserine, PE – phosphatidylethanolamine, PI – phosphatidylinositol, SM – sphingomyelin.

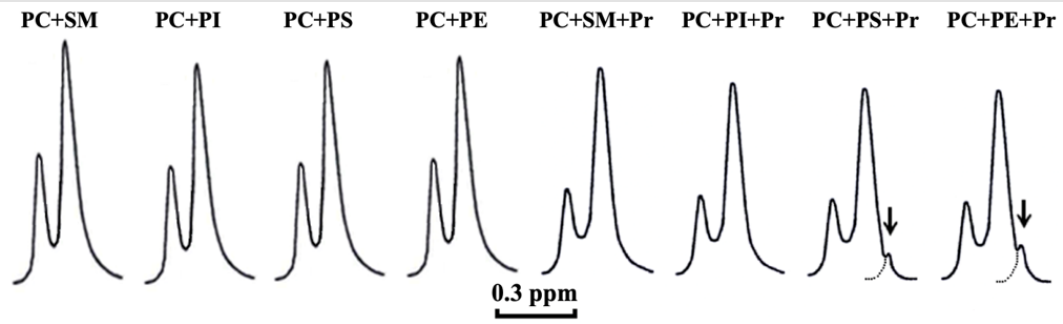

Figure 6: The ^{1}H-NMR signals derived from the protons of $N+(CH_3)_3$ groups of phosphatidylcholine and sphingomyelin in the outer and the inner monolayers of unilamellar liposomes modeling the four myelin membranes in the absence and presence of acidic and basic proteins (Pr) and in the presence of $K_3[Fe(CN)_3]$. The signal of smaller intensity in each ^{1}H-NMR spectrum comes from the inner monolayer while the signal of larger intensity comes from the outer monolayer. The total concentration of phospholipids and proteins in the samples is 1.4×10^{-2} M and 1.75×10^{-4} M respectively. The errors point at the signals from non-bilayer lipid phase. PC – phosphatidylcholine, PS – phosphatidylserine, PE – phosphatidylethanolamine, PI – phosphatidylinositol, SM – sphingomyelin.

Discussion

It has been suggested that physiologically active proteins in animal venom have evolved by mimicking the structure and functions of body proteins with important functional activity [42]. For example, many phospholipases isolated from snake and insect venoms resemble structurally and functionally the phospholipases that regulate inflammatory processes and lipid metabolism in biological membranes [42,43]. Rattlesnake venom metalloproteinases have been reported to act similarly to body metalloproteinases involved in controlling the homeostasis of blood and intercellular fluids [42,44]. Cationic proteins isolated from cobra venom have been shown to phenocopy the membranotropic activities of the C-8 protein from the Fo sector of ATP synthase [45-47]. In this research study, we present acidic and basic proteins isolated from the venom of the white widow spider Latrodectus pallidus, with amino acid sequences highly homologous to the isoforms of myelin basic proteins of the vertebrate central nervous system [25,26]. It is therefore reasonable to assume that the physiological activities of these acidic and basic proteins from Latrodectus pallidus venom resemble those of the myelin basic proteins of the vertebrate central nervous system.

Myelin basic proteins exist as isoforms that differ in size and charge [48]. The size isoforms are produced by alternative splicing of an mRNA transcript [49], while the charge isoforms result from post-translational modifications that decrease the basic charge, affecting the functional activities of the myelin basic proteins [26]. The size isoforms of human myelin basic proteins include proteins of 17.2, 18.5, 20.2, and 21.5 kDa, with the 18.5 kDa isoform being the most abundant and the most studied [26,49]. There are eight charge isoforms of the 18.5 kDa myelin basic protein, termed C1–C8. The C1 isoform has the highest positive charge and is the least modified after post-translational modification [26]. The charge isoforms C2–C6 are modified by phosphorylation, deamidation, and deamination, while C8 is predominantly modified by peptidyl arginine deiminase, which converts positively charged arginine to neutral citrulline. This conversion can involve up to 11 arginine residues, leading to an overall loss of positive charge of +11 [50]. The isoelectric points of the 18.5 kDa isoforms range from 4.5 for C8 to 11 for C1 [26], which is very similar to the isoelectric points of acidic and basic proteins of 18.5 kDa from the venom of the Latrodectus pallidus spider. This suggests that acidic and basic proteins from spider venom may phenocopy the functions of the C1 and C8 isoforms of the 18.5 kDa myelin basic protein.

The myelin sheath is a repetitive multilayer of tightly packed myelin membrane bilayers held together by proteins in myelin membranes [26]. The most long-lived proteins in the body are myelin basic proteins [51,52]. This suggests the importance of myelin basic proteins in the stability of the supramolecular structure of the myelin sheath [26]. It is believed that the C1 isoform functions by tightly attaching to acidic phospholipids of myelin bilayer membranes, stabilizing the tight packing of the myelin sheath [26]. Overall, C1, C2, and C3 are most likely responsible for myelin stability [26], while C8, which is abundant in childhood and scarce in adults, seems to play a role in development and is important in the formation of myelin rather than its stability [50]. However, the exact molecular mechanism of the functional role of C8 is not understood. Notably, the pathogenesis of multiple sclerosis (MS) is linked to abnormal changes in the 18.5 kDa isoform composition caused by an abnormal increase in the activity of peptidyl arginine deiminases, leading to the loosening of the tight packing of the myelin sheath [26,53-56].

The common explanation of the role of the myelin sheath is that it serves as an insulator of neuronal axons to promote rapid and saltatory conduction of nerve impulses [26,57]. However, nerve impulses are not transmitted through nerve fibers in the same way electrons move through a metal wire [57]. It is not clear how myelin insulates neurotransmission or what the insulation of nerve impulses means. It is obvious that even if myelin serves as an insulator in some way, it is far more than just an insulator [57]. A breakthrough discovery revealed aerobic ATP synthesis in the myelin sheath, which was unexpected as myelin is devoid of mitochondria [58-61]. However, oligomycin titration experiments have determined the presence of F1 subunits of ATP synthase in myelin [59], and the presence of respiratory complexes in lipid rafts of myelin was also established [62,63]. These discoveries suggest a way for delivering mitochondrial respiratory components to the lipid rafts in myelin.

Professor Alessandro Morelli of Genoa University proposed that mitochondria, which have their own DNA for respiratory complexes and ATP synthase to drive oxidative phosphorylation, deliver all the protein complexes necessary for ATP synthesis to the myelin sheath with the help of the endoplasmic reticulum (ER) [64], with which mitochondria are closely associated in cytoplasmic space and function [65,66]. It has been determined that mitochondria produce necessary vesicles providing the ER with the necessary oxidative phosphorylation complexes [67,68]. Aerobic ATP synthesis has also been observed in structures devoid of mitochondria such as rod outer segment discs [69-72], platelets [73], cell plasma membranes [74-78], exosomes, and microvesicles [79], strongly implying that the oxidative phosphorylation machinery is transferred to these extra-mitochondrial sites via the ER [80].

It has been shown by freeze-fracture X-ray crystallography that particles of 8.6 nm, the dehydrated F1 subunits of ATP synthases, are exposed on both sides of the myelin sheath [81,82]. This bi-faced orientation of F1 subunits in the myelin sheath does not agree with Mitchell's concept of delocalized proton coupling, where the gradient of proton concentrations in bulk water across the inner mitochondrial membrane drives the proton movement through ATP synthases with the F1 subunits exposed only on the matrix side. However, the orientation of F1 subunits on both sides of the myelin sheath agrees with the concept of localized coupling, where protons are absorbed and move along the surface on both sides of the myelin membrane, establishing a proton circuit built entirely inside a major dense line of myelin [80]. Professor Morelli suggests that extra-mitochondrial syn-

thesis of ATP can take place on any single membrane as long as the membrane surface can localize (absorb) protons to act as a 'proton capacitor', so the accumulated positive charge can support a proton circuit in which protons move along the membrane surface by the Grotthuss mechanism [83].

From the respiratory complexes to the F1 subunit of ATP synthase, and in the middle of the F1 subunit, protons turn to the hydrophobic center of the membrane through which protons move back to the respiratory complexes [23]. Thus, the proton circuit, taking place entirely inside a single membrane, couples respiration with ATP synthesis [23,64,80]. In our view, the experimental evidence described above supports localized proton coupling, which is based on the membrane's ability to absorb protons on its surface. However, we note that protons cannot move as charge through the low dielectric environment in the center of the membrane, and there must be a vehicle to transfer protons through the hydrophobic environment to the respiratory complexes.

The experimental results of our study on model myelin membranes with acidic and basic spider proteins, acting as isoforms of myelin basic proteins, showed that these membranes absorb protons on the membrane surface.

The protons are absorbed by both the phospholipid polar heads and the spider proteins, primarily by acidic proteins rather than basic ones. The ability of phospholipids to absorb protons differs depending on the physical-chemical properties of the phospholipid polar head. Additionally, we observed the formation of a non-bilayer phase in model myelin membranes made of PC+PS+Pr and PC+PE+Pr. We have previously observed the formation of a non-bilayer phase through the interaction of PS with basic proteins. The non-bilayer propensity of PE was also described previously, and it is strongly enhanced by interaction with basic proteins. Therefore, we can conclude that the non-bilayer phase in model myelin membranes was triggered by the interaction of spider basic protein, but not by spider acidic protein, with PS and PE. It should be noted that the highest ability to absorb protons was observed in PC+PS+Pr and PC+PE+Pr membranes, which contain the non-bilayer phase. In our previous studies, we have demonstrated that the non-bilayer phase in the inner mitochondrial membrane, triggered by basic proteins, stabilizes the intermembrane association between adjacent crista membranes, facilitating higher activity of ATP synthase [35,46,84,85].

One of the mechanisms for enhancing ATP synthase activity facilitated by the non-bilayer phase was recently proposed by us, in which inverted micelles transfer protons across the hydrophobic environment of the crista membrane in the inner aqueous volume of inverted micelles [35,86]. The non-bilayer phase observed in our study in model myelin membranes likely exists in the form of inverted micelles, which transport protons in the myelin membrane's hydrophobic environment, not across the membrane but through the membrane center from the F1 subunit to the respiratory complexes to complete the proton circuit inside a single membrane, as proposed by Professor Morelli [64,80].

Conclusion

The experimental results of our study support the new concept of the physiological role of the myelin sheath, related to the accumulation of energy through membrane action as a proton capacitor, as proposed by Professor A.M. Morelli. The stored energy is utilized for the production of ATP synthase through localized proton circuits that couple respiratory complexes with ATP synthases. According to Professor A.M. Morelli's proposal, the generated ATP molecules in the myelin sheath could be used by ionic pumps in neuronal axons for the rapid transmission of nerve impulses. Our results suggest that the acidic isoforms, but not the basic isoforms, of myelin basic proteins, along with phospholipid polar heads, are responsible for the absorption of protons on the membrane surface. Additionally, our results indicate that basic isoforms of myelin proteins interact with acidic PS and neutral PE to promote the formation of a non-bilayer phase. The non-bilayer phase may promote the tight association of adjacent myelin membranes and facilitate the transport of protons through the hydrophobic environment in the center of the myelin membrane to couple respiratory complexes with ATP synthase.

The results obtained in this study warrant further investigation of acidic and basic proteins from the Latrodectus pallidus spider venom in model myelin membrane systems. This research could lead to a better understanding of the molecular mechanisms of neurotransmission and neurodegeneration, as well as the potential development of novel pharmaceutical products that may alleviate or halt the process of myelin sheath degradation in aging and diseases.

Acknowledgement

Dr. Anwaar S Chaudary is grateful to Prof. L. Ya. Yukelson of the Institute of Biochemistry, Uzbekistan Academy of Sciences for Latrodectus pallidus spider venom given as a gift. The research project was supported by the start-up grant from the Beijing Chaoyang Kaiwen Academy to the STEM Research Center.

References

1. Guo R, Guo G, Wang A, Xu G, Lai R, et al. (2024) Spider-venom peptides: structure, bioactivity, strategy, and research applications. Molecules 29(1): 35.
2. Vassilevski A A, Irina M Fedorova, Ekaterina E Maleeva, Yuliya V Korolkova, Svetlana S Efimova, et al. (2010) Novel class of spider toxin: active principle from the yellow sac spider Cheiracanthium punctorium venom is a unique two-domain polypeptide. J Biol Chem 28(42): 32293-32302.
3. Vassilevski AA, Kozlov SA, Grishin EV (2009) Molecular diversity of spider venom. Biochemistry (Mosc) 74(13): 1505-1534.
4. Lewis RJ, Garcia ML (2003) Therapeutic potential of venom peptides. Nature Reviews Cancer 2(10): 790-802.
5. Olivera BM, G P Miljanich, J Ramachandran, M E Adams (1994) Calcium channel diversity and neurotransmitter release: the omega-conotoxins and omega-agatoxins. Annu Rev Biochem 63: 823-867.

6. Swartz K J (2007) Tarantula toxins interacting with voltage sensors in potassium channels. Toxicon 49(2): 213-230.
7. Windley MJ, Volker Herzig, Sławomir A Dziemborowicz, Margaret C Hardy, Glenn F King, et al. (2012) Spider-venom peptides as bioinsecticides. Toxins 4(3): 191-227.
8. Fitches E, Martin G Edwards, Christopher Me, Eugene Grishin, Angharad MR Gatehouse, et al. (2004) Fusion proteins containing insect-specific toxins as pest control agents: snowdrop lectin delivers fused insecticidal spider venom toxin to insect haemolymph following oral ingestion. J Insect Physiol 50(1): 61-71.
9. Ikonomopoulou M, King G (2013) Natural born insect killers: spider-venom peptides and their potential for managing arthropod pests. Outlook Pest Management 24(1): 16-19.
10. Valdez Mondragon A, Cabrera Espinoza LA (2023) Phylogenetic analyses and description of a new species of black widow spider of the genus Latrodectus Walckenaer (Araneae, Theridiidae) from Mexico; one or more species? European Journal of Taxonomy 897: 1-56.
11. Yan S, Wang X (2015) Recent advances in research on widow spider venoms and toxins. Toxins 7(12): 5055-5067.
12. Pires Jr OR, Fontes W, Castro MS (2015) Recent insights in Latrodectus ("black widow" spider) envenomation: toxins and their mechanisms of action. Spider Venoms.
13. Chen M, Daniel Blum, Lena Engelhard, Stefan Raunser, Richard Wagner, et al. (2021) Molecular architecture of black widow spider neurotoxins. Nat Commun 12(1): 6956.
14. Vetter R S, Isbister G K (2008) Medical aspects of spider bites. Annu Rev Entomol 53: 409-429.
15. Garb JE, Hayashi CY (2013) Molecular evolution of α-latrotoxin, the exceptionally potent vertebrate neurotoxin in black widow spider venom. Mol Biol Evol 30(5): 999-1014.
16. Ushkaryov YA, Volynski KE, Ashton AC (2004) The multiple actions of black widow spider toxins and their selective use in neurosecretion studies. Toxicon 43(5): 527-542.
17. Caruso MB, Pedro Santana Sales Lauria, Claudio Maurício Vieira de Souza, Luciana Lyra Casais-E-Silva, Russolina Benedeta Zingali (2021) Widow spiders in the New World: a review on Latrodectus Walckenaer, 1805 (Theridiidae) and latrodectism in the Americas. J Venom Anim Toxins incl Trop Dis 27: e20210011.
18. Holz GG, Habener JF (1998) Black widow spider alpha-latrotoxin: a presynaptic neurotoxin that shares structural homology with the glucagon-like peptide-1 family of insulin secretagogic hormones. Comparative Biochemistry and Physiology. Part B, Biochemistry & Molecular biology 121(2): 177-184.
19. Shatursky O Ya, V N Pashkov, O V Bulgacov, E V Grishin (1995) Interaction of α-latroinsectotoxin from Latrodectus mactans venom with bilayer lipid membranes. Biochim Biophys Acta 1233(1): 14-20.
20. Khamtorn P, Prapenpuksiri Rungsa, Nisachon Jangpromma, Sompong Klaynongsruang, Jureerut Daduang, et al. (2020) Partial proteomic analysis of brown widow spider (*Latrodectus geometricus*) venom to determine the biological activities. Toxicon X 8: 100062.
21. Wang Z, sen Zhu, Haorong Li, Lei Gao, Huanying Huang, et al. (2022) Chromosome-level genome assembly of the black widow spider Latrodectus elegans illuminates composition and evolution of venom and silk proteins. GigaScience 11: 1-11.
22. Chaudary AS (2014) Isolation and sequence determination of acidic and basic proteins from the Latrodectus pallidus spider venom. FAN, Tashkent.
23. Morelli A M, Ravera S, Calzia D, Panfoli I (2019) An update of the chemiosmotic theory as suggested by possible proton currents inside the coupling membrane. Open Biol 9: 180221.
24. Crestfield A M, S Moore, WH stein (1963) The preparation and enzymatic hydrolysis of reduced and S-carboxymethylated proteins. J Biol Chem 238: 622-627.
25. Grishin EV, AP Sukhikh, NN Lukyanchuk, LN Slobodyan, VM Lipkin, et al. (1973) Amino acid sequence of neurotoxin II from Naja naja oxiana venom. FEBS Letters 36(1): 77-78.
26. Martinsen V, Kursula P (2022) Multiple sclerosis and myelin basic protein: insights into protein disorder and disease. Amino Acids 54(1): 99-109.
27. Raasakka A, Salla Ruskamo, Julia Kowal, Robert Barker, Anne Baumann, et al. (2017) Membrane association landscape of myelin basic protein portrays formation of the myelin major dense line. Sci Rep 7: 4974.
28. Fewster M E, Hirono H, Mead J F (1976) Lipid composition of myelin in multiple sclerosis. J Neurol 213(2): 119-131.
29. Neu I, Woelk H (1982) Investigations of the lipid metabolism of the white matter in multiple sclerosis Changes in glycero-phosphatides and lipid-splitting enzymes. Neurochem Res 7: 727-735.
30. Del Boccio P, Damiana Pieragostino, Maria Di Ioia, Francesca Petrucci, Alessandra Lugaresi, et al. (2011) Lipidomic investigations for the characterization of circulating serum lipids in multiple sclerosis. J Proteomics 74(12): 2826-2836.
31. Göpfert E, Pytlik S, Debuch H (1980) 2′,3′-Cyclic nucleotide 3′-phosphohydrolase and lipids of myelin from multiple sclerosis and normal brains. J Neurochem 34(3): 732-739.
32. Valdivia AO, Farr V, Bhattacharya S K (2019) A novel myelin basic protein transcript variant in the murine central nervous system. Mol Biol Rep 46(2): 2547-2553.
33. Valdivia AO, KePratul K Agarwal, Sanjoy K Bhattacharya (2020) Myelin basic protein phospholipid complexation likely competes with deimination in experimental autoimmune encephalomyelitis mouse model. ACS Omega 5(25): 15454-15467.
34. Van der Veen J N, John P Kennelly, Sereana Wan, Jean E Vance, Dennis E Vance, et al. (2017) The critical role of phosphatidylcholine and phosphatidylethanolamine metabolism in health and disease. Biochim Biophys Acta, pp. 1558-1572.
35. Li M, Gasanoff E S (2023) Cationic proteins rich in lysine residue trigger formation of non-bilayer lipid phases in model and biological membranes: Biophysical methods of study. J Membrane Biol 256(4-6): 373-391.
36. Li F, Shrivastava I H, Hanlon P, Dagda R K, Gasanoff E S (2020) Molecular mechanism by which cobra venom cardiotoxins interact with the outer mitochondrial membrane. Toxins (Basel) 12(7): 425.
37. Wang H, Qin H, Garab G, Gasanoff ES (2022) Short-chained alcohols make membrane surfaces conducive for melittin action: implication for the physiological role of alcohols in cells. Cells (Basel) 11(12): 1928.
38. Gasanov SE, Shrivastava IH, Israilov FS, Kim AA, Rylova KA, et al. (2015) Naja naja oxiana cobra venom cytotoxins CTI and CTII disrupt mitochondrial membrane integrity: Implications for basic three-fingered cytotoxins. PLoS ONE 10(6): e0129248.
39. Gasanov SE, Alsarraj MA, Gasanov NE, Rael E D (1997) Cobra venom cytotoxin free of phospholipase A2 and its effect on model membrane and T leukemia cells. J Membr Biol 155(2): 133-142.
40. Gasanov SE, Salakhutdinov BA, Aripov TF (1990) Formation of nonbilayer structures in phospholipid membranes induced by cationic polypeptides. Biol Membr 7: 1045-1055.

41. Gasanov S E, Vernon L P, Aripov T F (1993) Modification of phospholipid membrane structure by the plant toxic peptide *Pyrularia thionin*. Arch Biochem Biophys 301: 367-374.

42. Gasanov S E, Dagda R K, Rael E D (2014) Snake venom cytotoxins, phospholipase A_2s, and Zn^{+2}-dependent metalloproteinases: Mechanisms of action and pharmacological relevance. J Clin Toxicol 4(1): 1000181.

43. Gasanov S E, Rael E D, Martinez M, Baeza G, Vernon L P (1994) Modulation of phospholipase A_2 activity by membrane-active peptides on liposomes of different phospholipid composition. Gen Physiol Biophys 13(4): 275-286.

44. Dagda R K, Gasanov S E, Ysidro De La Oiii, Eppie D Rael, Carl S Lieb (2013) Genetic basis for variation of metalloproteinase-associated biochemical activity in venom of the Mojave rattlesnake (*Crotalus scutulatus scutulatus*). Biochem Res Intr.

45. Gasanov S E, Kim A A, Dagda R K (2016) The possible role of nonbilayer structures in regulating ATP synthase activity in mitochondrial membranes. Biophysics (oxf) 61(4): 596-600.

46. Gasanov S E, Kim A A, Yaguzhinsky L S, Dagda R K (2018) Non-bilayer structures in mitochondrial membranes regulate ATP synthase activity. Biochim Biophys Acta 1860(2): 586-599.

47. Gasanov S E, Kim A A, Dagda R K (2016) Possible role of nonbilayer structures in regulating the activity of ATP synthase in mitochondria. Biofizika 61: 705-710.

48. Vassall K A, Bamm VV, Harauz G (2015) MyelStones: the executive roles of myelin basic protein in myelin assembly and destabilization in multiple sclerosis. Biochem J 472: 17-32.

49. Boggs J M (2006) Myelin basic protein: a multifunctional protein. Cell Mol Life Sci 63(7): 1945-1961.

50. Wood D D, Moscarello MA (1989) The isolation, characterization, and lipid-aggregating properties of a citrulline containing myelin basic protein. J Biol Chem 264(9): 5121-5127.

51. Toyama B H, Jeffrey N Savas, Sung Kyu Park, Michael S Harris, Nicholas T Ingoli, et al (2013) Identification of long-lived proteins reveals exceptional stability of essential cellular structures. Cell 154(5): 971-982.

52. Fornasiero E F, Sunit Mandad, Hanna Wildhagen, Mihai Alevra, Burkhard Rammner, et al. (2018) Precisely measured protein lifetimes in the mouse brain reveal differences across tissues and subcellular fractions. Nat Commun 9(1): 4230.

53. Beniac DR, DD Wood, N Palaniyar, FP Ottensmeyer, MA Moscarello, et al. (1999) Marburg's variant of multiple sclerosis correlates with a less compact structure of myelin basic protein. Mol Cell Biol Res Commun 1: 48-51.

54. Boggs J M, G Rangaraj, KM Koshy, C Ackerley, DD Wood, et al (1999) Highly deiminated isoform of myelin basic protein from multiple sclerosis brain causes fragmentation of lipid vesicles. J Neurosci Res 57(4): 529-535.

55. Wood DD, Bilbao JM, O'Connors P, Moscarello MA (1996) Acute multiple sclerosis (Marburg type) is associated with developmentally immature myelin basic protein. Ann Neurol 40: 18-24.

56. Valdivia A O, Pratul K Agarwal, Sanjoy K Bhattacharya (2020) Myelin basic protein phospholipid complexation likely competes with deimination in experimental autoimmune encephalomyelitis mouse model. ACS Omega 5(25): 15454-15467.

57. Fields R D (2014) Myelin – more than insulation. Science 344(6181): 264-266.

58. Ravera S, Isabella Panfoli, Daniela Calzia, Maria Grazia Aluigi, Paolo Bianchini, et al. (2009) Evidence for aerobic ATP synthesis in isolated myelin vesicles. Int J Biochem Cell Biol 41(7): 1581-1591.

59. Morelli A, Ravera S, Panfoli I (2011) Hypothesis of an energetic function for myelin. Cell Biochem Biophys 61(1): 179-187.

60. Ravera S, Martina Bartolucci, Patrizia Garbati, Sara Ferrando, Daniela Calzia, et al. (2016) Evaluation of the acquisition of the aerobic metabolic capacity by myelin, during its development. Mol Neurobiol 53(10): 7048-7056.

61. Bartolucci M, Silvia Ravera, Greta Garbarino, Paola Ramoino, Sara Ferrando, et al. (2015) Functional expression of electron transport chain and FoF1-ATP synthase in optic nerve myelin sheath. Neurochem Res 40(11): 2230-2241.

62. Panfoli I, Ravera S, Bruschi M, Candiano G, Morelli A (2011) Proteomics unravels the exportability of mitochondrial respiratory chains. Exp Rev Proteomics 8(2): 231-239.

63. Lee A G (2001) Myelin: delivery by raft. Curr Biol 11(2): R60-R62.

64. Morelli A M (2022) A new way of understanding bioenergetics. Biology 142: 66-69.

65. Lee S, Min K-T (2018) The interface between ER and mitochondria: molecular compositions and functions. Mol Cells 41(12): 1000-1007.

66. Marchi S, Patergnani S, Pinton P (2014) The endoplasmic reticulum-mitochondria connection: one touch, multiple functions. Biochim Biophys Acta 1837(4): 461-469.

67. Ravera S, Martina Bartolucci, Daniela Calzia, Alessandro M Morelli, Isabella Panfoli (2021) Efficient extra-mitochondrial aerobic ATP synthesis in neuronal membrane systems. J Neurosci Res 99(9): 2250-2260.

68. Morelli A M, Scholkmann F (2024) Should the standard model of cellular energy metabolism be reconsidered? Possible coupling between the pentose phosphate pathway, glycolysis and extra-mitochondrial oxidative phosphorylation. Biochimie 221: 99-109.

69. Calzia D, Simona Candiani, Greta Garbarino, Federico Caicci, Silvia Ravera, et al. (2013) Are rod outer segment ATP-ase and ATP-synthase activity expression of the same protein? Cell Mol Neurobiol 33(5): 637-649.

70. Bianchini P, Daniela Calzia, Silvia Ravera, Giovanni Candiano, Angela Bachi, et al. (2008) Live imaging of mammalian retina: rod outer segments are stained by conventional mitochondrial dyes. J Biomed Opt 13(5): 054017.

71. Panfoli I, Daniela Calzia, Paolo Bianchini, Silvia Ravera, Alberto Diaspro, et al. (2009) Evidence for aerobic metabolism in retinal rod outer segment disks. Int J Biochem Cell Biol 41(12): 2555-2565.

72. Calzia D, Greta Garbarino, Federico Caicci, Lucia Manni, Simona Candiani, et al. (2014) Functional expression of electron transport chain complexes in mouse rod outer segments. Biochimie 102: 78-82.

73. Ravera S, Maria Grazia Signorello, Martina Bartolucci, Sara Ferrando, Lucia Manni, et al. (2018) Extramitochondrial energy production in platelets. Biol Cell 110(5): 97-108.

74. Taurino F, Caterina Giannoccaro, Anna Maria Sardanelli, Alessandro Cavallo, Elisa De Luca, et al. (2016) Function and expression study uncovered hepatocyte plasma membrane ecto-ATP synthase as a novel player in liver regeneration. Biochem J 473(16): 2519-2530.

75. Gao J, Tian Zhang, Zhanfang Kang, Weijen Ting, Lingqing Xu, et al. (2017) The F0F1 ATP synthase regulates human neutrophil migration through cytoplasmic proton extrusion coupled with ATP generation. Mol Immunol 90: 219-226.

76. Lee H, Seung-Hyeob Kim, Jae-Seon Lee, Yun-Hee Yang, Jwa Min Nam, et al. (2016) Mitochondrial oxidative phosphorylation complexes exist in the sarcolemma of skeletal muscle. BMB Rep 49(2): 116-121.

77. Taurino F, Gnoni A (2018) Systematic review of plasma-membrane ecto-ATP synthase: a new player in health and disease. Exp Mol Pathol 104(1): 59-70.

78. Kita T, Arakaki N (2015) Contribution of extracellular ATP on the cell-surface F1F0-ATP synthase-mediated intracellular triacylglycerol accumulation. Biomed Res 36(2): 115-120.

79. Panfoli I, Silvia Ravera, Marina Podestà, Claudia Cossu, Laura Santucci, et al. (2016) Exosomes from human mesenchymal stem cells conduct aerobic metabolism in term and preterm newborn infants. FASEB J 30(4): 1416-1424.

80. Morelli A M, Ravera S, Panfoli I (2020) The aerobic mitochondrial ATP synthesis from a comprehensive point of view. Open Biol 10(10): 2000224.

81. Gabriel G, P K Thomas, R H King, C Stolinski, A S Breathnach (1986) Freeze-fracture observations on human peripheral nerve. J Anat 146: 153-166.

82. Surchev L, Ichev K, Dolapchieva S (1992) A freeze-etch study of the central myelin. Rom J Morphol Embryol 38(3-4): 77-80.

83. Fischer S A, Gunlycke D (2019) Analysis of correlated dynamics in the Grotthuss mechanism of proton diffusion. J Phys Chem B 123(26): 5536-5544.

84. Gasanoff ES, Yaguzhinsky LS, Garab G (2021) Cardiolipin, non-bilayer structures and mitochondrial bioenergetics: relevance to cardiovascular disease. Cells 10(7): 1721.

85. Garab G, Yaguzhinsky L S, Dlouhý O, Nesterov S V, Špunda V, et al. (2022) Structural and functional roles of non-bilayer lipid phases of chloroplast thylakoid membranes and mitochondrial inner membranes. Prog Lip Res 86: 101163.

86. Han Y, Tao Y, Gasanoff E S (2023) Non-bilayer lipid phases modulate the structure and functions of mitochondrial membranes: Pharmacological relevance. Am J Biomed Sci Res 19(5): 646-659.

ISSN: 2574-1241

DOI: 10.26717/BJSTR.2024.56.008895

Edward S Gasanoff. Biomed J Sci & Tech Res

Submission Link: https://biomedres.us/submit-manuscript.php